

Preparation of Unsupported NiMoP Catalysts for 4,6-Dimethyldibenzothiophene Hydrodesulfurization

Rui Wang · Kevin J. Smith

Received: 7 March 2014 / Accepted: 27 May 2014
© Springer Science+Business Media New York 2014

Abstract The preparation of unsupported NiMoP catalysts in the presence of citric acid (CA) is reported. Phase pure NiMoP with a surface area ~ 60 m²/g was synthesized in the presence of CA at low reduction temperature (550 °C), with a Ni/Mo/P molar ratio of 1/1/1 and a 1.5 CA/Me ratio (Me = Ni + Mo). Depending on the synthesis conditions, small amounts of MoP and NiMoP₂ were also present in the catalysts. The catalyst precursors appeared similar to those identified for MoP and Ni₂P catalysts, also synthesized in the presence of CA. For the phase pure NiMoP catalysts, the TOFs for the HDS of 4,6-dimethyldibenzothiophene were almost identical, despite large differences in NiMoP surface area and crystallite size.

Keywords Heterogeneous catalysis · Hydrodesulfurization · Metal phosphide · Catalyst preparation · Environmental catalysis

1 Introduction

Transition metal phosphides are viewed as an alternative class of catalysts that have potential for ultra-deep hydrodesulfurization (HDS) and hydrodenitrogenation (HDN) of petroleum feedstocks [1–3]. Both unsupported and supported metal phosphides can be prepared by temperature-programmed reduction (TPR) of the corresponding metal phosphate salts [1, 4]. Recent studies have reported on the synthesis of high surface area, unsupported monometallic phosphides (MoP and Ni₂P) by adding citric acid

(CA) to precursor metal salt solutions, prior to TPR [5, 6]. The citric acid acts as a chelating agent, yielding Ni or Mo citrate complexes that control crystallization during calcination and TPR [7].

Although Ni and Co are effective promoters of MoS₂ hydrotreating catalysts [8–10] their impact is quite different in the case of metal phosphides. Sun et al. [11] reported that the dibenzothiophene HDS activity of phosphide catalysts followed the order Ni₂P/SiO₂ > NiMoP/SiO₂ > MoP/SiO₂, with no synergistic effect observed between the Ni and Mo, unlike with sulfides, nitrides, and carbides. Similar results were reported for the hydrodeoxygenation (HDO) of anisole by Li et al., wherein the HDO activities decreased in the order Ni₂P/SiO₂ > NiMoP/SiO₂ > MoP/SiO₂ [12]. Others have reported enhanced activities of bimetallic phosphides but the catalyst activity is very dependent upon composition [13]. For example, in a previous study of Ni_xMoP catalysts, in which Ni was added to MoP to give a Ni/Mo ratio from 0.125 to 1, the initial conversion of 4,6-dimethyldibenzothiophene over Ni_xMoP catalysts was lower than that of MoP, and this was attributed to an increased crystallite size of MoP and NiMoP [5, 6]. In contrast, the turnover frequency (TOF) of the Ni_xMoP catalysts increased linearly with increased Ni content and the Ni_xMoP catalysts were shown to be a mixture of MoP and NiMoP.

In the present paper, we report on the effect of various preparation conditions on the properties of unsupported NiMoP catalysts. As before, the catalysts were prepared in the presence of CA to obtain high surface area, but in this case the Ni:Mo molar ratio was fixed at 1:1. Variables investigated include the amount of CA used in the preparation of the precursor salts, the precursor composition, and the reduction temperature. The relationship between these variables, the resultant NiMoP structure and the HDS activity, is reported.

R. Wang · K. J. Smith (✉)
Department of Chemical and Biological Engineering, University of British Columbia, Vancouver, BC V6T 1Z3, Canada
e-mail: kjs@mail.ubc.ca

2 Experimental

2.1 Catalyst Preparation

The unsupported NiMoP catalysts were prepared by first dissolving required amounts of $(\text{NH}_4)_6\text{Mo}_7\text{O}_{24}\cdot 4\text{H}_2\text{O}$, $(\text{NH}_4)_2\text{HPO}_4$ and citric acid in 15 ml of water. A second solution was prepared by dissolving an appropriate amount of $\text{Ni}(\text{NO}_3)_2\cdot 6\text{H}_2\text{O}$ and citric acid in 15 ml of deionized water. The two solutions were then mixed so that the final solution contained the required CA/Me ratio (Me = Mo + Ni), and the synthesis yielded 2–5 g of catalyst precursor. Various formulations of the precursor solutions were investigated, but in all cases the Ni/Mo molar ratio was 1. Catalysts denoted as NiMoP-xP, where x represents the P/Me molar ratio, were prepared with P/Me ratios of 1, 0.75 and 0.5 and a fixed CA/Me molar ratio of 1. A second series of catalysts, denoted as NiMoP-xCA, where x represents the CA/Me molar ratio, were prepared with CA/Me ratios of 1.5, 1, 0.75 and 0.5 and a fixed P/Me molar ratio of 1. In each case, the precursor solution was aged in a covered beaker in a water bath held at 90 °C for 24 h. The resulting gel was dried in an oven at 120 °C for 24 h and this material is referred to as the dried catalyst precursor. Subsequently the dried precursor was calcined at 500 °C for 5 h, cooled and ground to a powder ($d_p < 0.7$ mm). This material is referred to as the calcined catalyst precursor. The active metal phosphide was subsequently obtained by temperature-programmed reduction (TPR) of the calcined precursor in H_2 (Praxair, 99.99 %) at a flow rate of 160 ml(STP)/min. A heating rate of 5 °C/min to 300 °C, followed by a heating rate of 1 °C/min to the final reduction temperature was used for the TPR, with the final temperature held for 2.5 h. Final reduction temperatures of 500–650 °C were examined for the NiMoP-0.75CA catalyst, whereas all other catalysts were reduced to 650 °C. The reduced catalyst was cooled to room temperature in He and passivated in a flow of 1 % O_2/He for 3 h at room temperature prior to removal from the reactor. This material is referred to as the passivated catalyst. Table 1 lists the catalyst compositions, calcination temperatures and reduction temperatures examined in the synthesis of unsupported NiMoP catalysts in the present study. For comparison, we also prepared an unsupported NiMoP catalyst without citric acid using the conventional TPR method to reduce the corresponding phosphate precursor.

2.2 Catalyst Characterization

The chemical composition of the catalysts was determined using inductively coupled plasma-atomic emission spectroscopy (ICP-AES, done by Cantest Laboratories, Vancouver, BC). Powder X-ray diffraction (XRD) analyses

Table 1 List of preparation conditions used in the present study for high surface area NiMoP synthesis

Sample	P/Me molar ratio	CA/Me molar ratio	Reduction temperature (°C)
NiMoP-1P	1.0	1.0	650
NiMoP-0.75P	0.75	1.0	650
NiMoP-0.5P	0.5	1.0	650
NiMoP-1.5CA	0.5	1.5	650
NiMoP-1CA	0.5	1.0	650
NiMoP-0.75CA	0.5	0.75	650
NiMoP-0.5CA	0.5	0.5	650
NiMoP-noCA	0.5	0	650
NiMoP-650	0.5	0.75	650
NiMoP-600	0.5	0.75	600
NiMoP-550	0.5	0.75	550

All catalysts calcined at 500 °C

were performed on the dried and calcined catalyst precursors and the passivated catalysts using a Siemens D500 diffractometer with $\text{Cu K}\alpha$ X-rays ($\lambda = 1.54$ Å). Phase identification was carried out after subtraction of the background and the grain size of selected phases was calculated from the diffractograms using the Scherrer equation with correction for instrument broadening.

Diffuse reflectance infrared Fourier-transform (DRIFT) spectroscopy measurements were performed on a Thermo Scientific Nicolet iS10 Fourier transform IR spectrometer equipped with a MCT detector and a high temperature/high pressure chamber. The sample was diluted with KBr and DRIFTS spectra were collected from 650 to 4,000 cm^{-1} at a resolution of 2 cm^{-1} averaged over 35 scans, in a N_2 atmosphere at room temperature.

N_2 adsorption–desorption isotherms, measured at -196 °C using a Micromeritics ASAP 2020 unit, were used to determine the BET surface area and pore volume of the catalysts. The passivated catalysts were degassed at 250 °C for 10 h prior to the measurement. TPR experiments were carried out using a Micromeritics AutoChem II 2920 system. Prior to TPR the calcined catalyst was pretreated in Ar at 500 °C for 1 h, and then cooled to room temperature. Subsequently, the Ar flow was switched to 10 % H_2/Ar and the sample was heated from room temperature to 1,000 °C at a rate of 5 °C/min. The H_2 consumption was measured by a thermal conductivity detector (TCD).

The CO uptake was measured by pulsed chemisorption also using the Micromeritics Autochem II 2920. The

passivated catalyst was pretreated to remove the passivation layer by passing 50 ml(STP)/min of 10 % H₂/Ar while heating from 40 to 650 °C at a rate of 5 °C/min, maintaining the final temperature for 1 h. The 10 % H₂/Ar flow was then switched to He (50 ml(STP)/min) at 650 °C for 1 h in order to remove adsorbed species. The reactor was subsequently cooled to 25 °C, and 0.5 ml pulses of CO were injected into a flow of He (50 ml(STP)/min) and the CO uptake was measured using a TCD. CO pulses were repeatedly injected until no further CO uptake was observed after consecutive injections.

A Leybold Max200 X-ray photoelectron spectrometer was used for XPS analysis of the catalysts. Al K α was used as the photon source generated at 15 kV and 20 mA. The pass energy was set at 192 eV for the survey scan and 48 eV for the narrow scan. All catalyst samples were analysed after passivation at room temperature. Exposure of the samples to ambient atmosphere was minimized by transferring the samples either in vacuum or under N₂. All XPS spectra were corrected to the C1s peak at 285.0 eV.

2.3 Catalyst Activity

The HDS of 4,6-dimethyldibenzothiophene (4,6-DMDBT) was measured in a fixed bed reactor (i.d. = 9 mm) at 310 °C and 3.0 MPa H₂. The passivated catalysts ($d_p < 0.7$ mm) were activated at 600 °C for 1 h in H₂ at a flow rate of 160 ml(STP)/min prior to the reaction. The concentration of 4,6-DMDBT was 3,000 ppm in toluene. The liquid feed was evaporated into a stream of flowing H₂. Gas and liquid flows and catalyst charged to the reactor were chosen to give a WHSV = 26 h⁻¹. The product was collected periodically and analyzed using a Varian Star 3400 Gas Chromatograph equipped with a flame ionization detector (FID). Component separation was achieved using a capillary column (CP-Sil 19 CB, 25 m length and 0.53 mm i.d.). Component identification was confirmed using the same column and a GC-MS (Agilent 6890/5973N).

For all the activity data reported herein, the carbon balance across the reactor was >95 % and a number of the experiments were repeated to ensure repeatability of the data.

3 Results and Discussion

3.1 Catalyst Characterization

The XRD analysis of the passivated NiMoP catalysts (Figs. 1, 2, 3) showed the presence of a NiMoP phase mixed with varying amounts of MoP. For the NiMoP catalysts prepared with different P/Me ratios (see Fig. 1) a

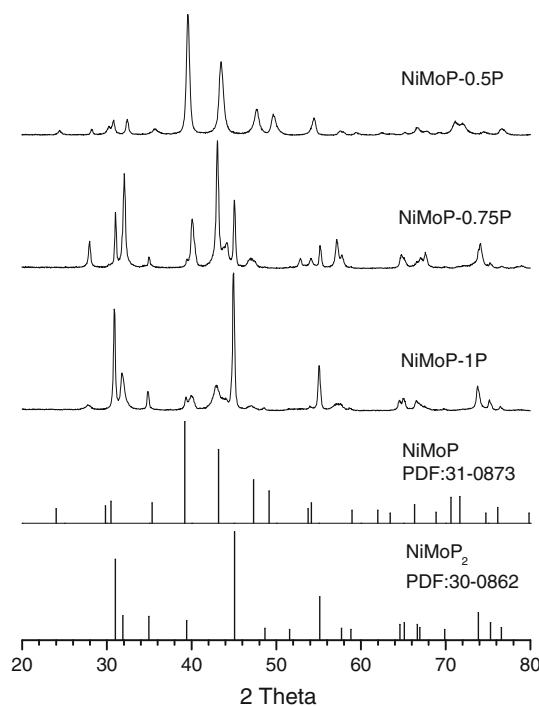


Fig. 1 X-ray diffractograms of NiMoP passivated catalysts prepared with varying P/Me ratios

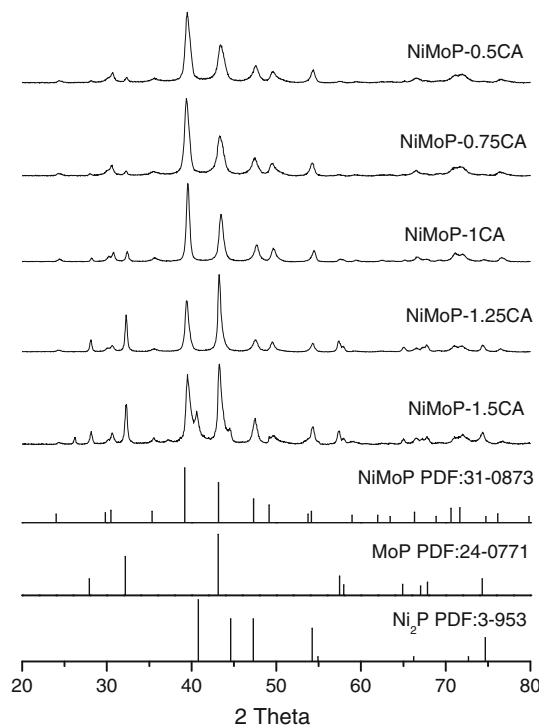


Fig. 2 X-ray diffractograms of NiMoP passivated catalysts prepared with varying CA/Me ratios

new P-rich NiMoP₂ phase appeared at increased P concentrations. The NiMoP₂ was dominant for the NiMoP-1P catalyst. Lee et al. [14] also reported the presence of

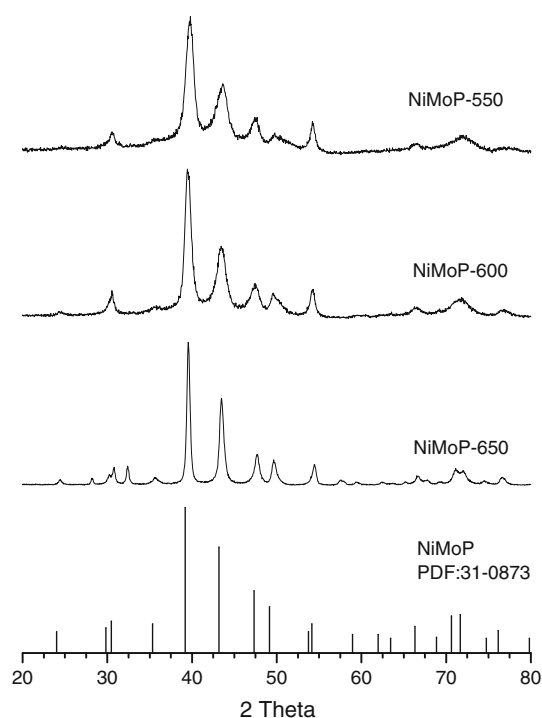


Fig. 3 X-ray diffractograms of NiMoP passivated catalysts prepared with varying reduction temperatures

NiMoP₂ in excess P (Ni/Mo/P = 1/1/2.5). For the NiMoP-xP catalysts, the grain size of MoP, as determined from the XRD analysis, decreased from 32 to 14 nm as the P content increased, while the grain size of NiMoP₂ (45 nm) was not affected by increased P content (Table 2). Moreover, the surface areas significantly increased with P content. These data suggest that growth of MoP domains was inhibited by the Ni and excess P, likely due to the decoration of Ni and P on the edges of MoP crystallites.

Figure 2 shows the XRD patterns of the NiMoP catalysts prepared with different CA/Me ratios (NiMoP-xCA catalysts prepared with P/Me = 0.5 and a final reduction temperature of 650 °C). In all cases NiMoP was the dominant phase and as the CA content increased, the peaks associated with MoP and NiMoP sharpened, indicative of increased crystallization. For NiMoP prepared without citric acid (NiMoP-noCA), similar diffractograms were obtained [5]. The grain size of NiMoP-xCA, reported in Table 2, increased from 12 to 25 nm as the CA content increased. The surface areas, also shown in Table 2, were higher than that of NiMoP-noCA, and reached a maximum of 40 m²/g at a CA/Me ratio of 0.75. The maximum in surface area with CA content was likely due to residual carbon in the catalyst [7] and is in agreement with similar trends observed for Ni₂P and MoP catalysts prepared with CA [7, 15]. Note that for the NiMoP-1.5CA, a new Ni₂P phase appeared (Fig. 2), implying that excess citric acid restricts Ni-Mo interaction. This effect is likely related to

Table 2 Textural and crystalline properties of NiMoP catalysts prepared by TPR of calcined precursor salts mixed with citric acid (CA)

Sample	XRD		BET (m ² /g)	Pore volume (cm ³ /g)	Average pore size (nm)
	Phase	Grain size (nm)			
NiMoP-1P	MoP, NiMoP ₂	14, 44	66	0.04	3.3
NiMoP-0.75P	MoP, NiMoP ₂	26, 45	78	0.09	4.6
NiMoP-0.5P	MoP, NiMoP	32, 24	16	0.03	70
NiMoP-1.5CA	MoP, NiMoP, Ni ₂ P	31, 25, 60	9	0.02	8.8
NiMoP-1CA	MoP, NiMoP	32, 24	16	0.03	70
NiMoP-0.75CA	MoP, NiMoP	31, 16	40	0.04	43
NiMoP-0.5CA	MoP, NiMoP	24, 12	24	0.05	86
NiMoP-noCA	MoP, NiMoP	31, 19	8	0.02	8.7
NiMoP-650	MoP, NiMoP	31, 16	40	0.04	43
NiMoP-600	NiMoP	11	35	0.05	59
NiMoP-550	NiMoP	9	58	0.05	35

the different metal citrate precursors formed from the (NH₄)₆Mo₇O₂₄·4H₂O and Ni(NO₃)₂·6H₂O salts, as discussed previously [7].

The X-ray diffractograms of the NiMoP catalysts, prepared using different final reduction temperatures, are shown in Fig. 3. For the NiMoP-650 sample, a mixture of MoP and NiMoP was observed, similar to the mixed MoP and NiMoP phase reported by Stinner et al. [4], although Ma et al. [16] reported that phase pure NiMoP was obtained from a precursor with Ni/Mo/P = 1 when a high H₂ flow rate (1,000 ml/min) was used in the TPR. Figure 3 shows that a lower final reduction temperature favored the production of phase pure NiMoP with broad diffraction peaks, indicative of smaller crystallites. The NiMoP grain size increased from 9 to 16 nm with increased reduction temperature from 550 to 650 °C, while the surface area decreased from 58 to 40 m²/g (Table 2). From these results one concludes that phase pure, high surface area NiMoP can be obtained at lower reduction temperature (550 °C), with a Ni/Mo/P ratio of 1/1/1 and a 1.5 CA/Me ratio (Me = Ni + Mo).

For the NiMoP-noCA catalyst, a green precipitate was formed immediately that the Ni or Mo salt was mixed with the (NH₄)₂HPO₄ solution. However, for the NiMoP-xCA samples, a green gel-like product formed during mixing and the viscosity of the gel increased with increased CA content. During drying at 120 °C, water was further removed and a foam-like maroon material was produced.

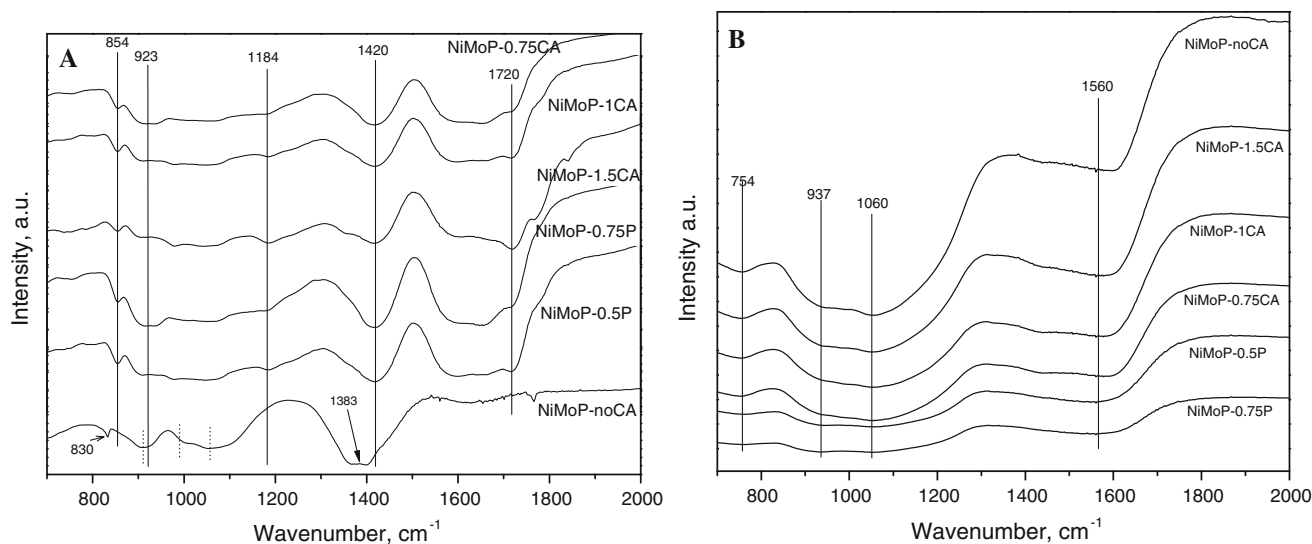


Fig. 4 DRIFT spectra of NiMoP dried precursors (**a**) and calcined precursors (**b**)

Figure 4 shows the DRIFT spectra of the dried NiMoP-xCA, NiMoP-xP and NiMoP-noCA catalyst precursors. For the dried NiMoP-noCA (Fig. 4a), three bands at 920, 989 and 1,053 assigned to metal ammonia phosphate complexes (i.e., PO_4^{3-} , HPO_4^{2-}) are apparent, and a decrease in intensity of these bands was observed with an increase in the amount of CA used in the preparation. The band at 830 cm^{-1} is assigned to NiMoO_4 , suggesting that a portion of the Ni and Mo did not interact with the P [14]. The sharp band at $1,383\text{ cm}^{-1}$ is ascribed to NO_3^- [17]. For the NiMoP-xCA catalysts, the characteristic peak of bimetallic oxides or nitrate at 830 and $1,383\text{ cm}^{-1}$ both disappeared, demonstrating that chelating of the Mo or Ni atom with citric acid could break the polyanionic cluster. New bands at 854 , $1,184$ and $1,420\text{ cm}^{-1}$ assigned to metal citrates were observed, indicating that carboxyl hydrogen was replaced by Ni or Mo to form citrate complexes [7]. In addition, a new band at $1,720\text{ cm}^{-1}$ assigned to the free C=O of carboxylic acid [7, 18] in citric acid, appeared and its intensity increased with increased CA content. It follows therefore that only a fraction of the H atoms associated with -COOH were replaced by the metal. Hence we conclude that the dried NiMoP-xCA precursors were composed of a metal citrate complex, phosphomolybdate, and nonbonded citric acid, similar to what was observed during the synthesis of the mono-metal phosphides MoP and Ni_2P using CA [7, 15]. For the NiMo-xP catalysts (Fig. 4a), the intensity of the bands at ~ 923 , $1,080$ and $1,180\text{ cm}^{-1}$ associated with phosphate complexes (i.e., PO_4^{3-} , HPO_4^{2-}) [19], increased with increased P content. The intensity of a series of characteristic peaks of the metal citrates (854 and $1,420\text{ cm}^{-1}$) also increased with increased P content, suggesting that the interaction between phosphates and metal citrate increased with P content.

The calcined NiMoP-noCA and NiMoP-xCA precursors were quite different in appearance, with the former a dense green precipitate, whereas the latter was brown in colour with low density and high porosity, apparently due to organic residues [7]. The FTIR spectra of the calcined NiMoP-xCA and NiMoP-xP catalyst precursors are shown in Fig. 4b. Compared with the spectra of the dried samples, the bands corresponding to phosphates, citrate groups and citric acid completely disappeared after calcination. The Mo-O-Mo vibration at 754 cm^{-1} of the calcined NiMoP-xCA was weaker than that of the calcined NiMoP-noCA suggesting that the precursors prepared in the presence of CA reduced the degree of Mo aggregation. The broad region from 930 to $1,100\text{ cm}^{-1}$ is composed of Ni(Mo)-P-O heteropoly compounds containing P-O bonded with Mo and/or Ni.

The DRIFTS features following drying and calcination of the NiMoP catalyst precursors were very similar to those reported previously for the Ni_2P and MoP samples, also prepared with CA [7, 15]. These data suggest that the formation of NiMoP follows from chemically similar precursors as were identified for the synthesis of Ni_2P and MoP in the presence of CA [7, 15].

The TPR profiles of the NiMoP-xCA calcined catalyst precursors are shown in Fig. 5. The reduction peak temperature of all samples ($\sim 620\text{ }^\circ\text{C}$) was much lower than that of MoP ($712\text{ }^\circ\text{C}$) or Ni_2P ($721\text{ }^\circ\text{C}$) prepared with CA, as reported previously [5]. Similar TPR profiles containing one shoulder and one main peak assigned to Ni-Mo-O and Ni-Mo-O-P precursors, respectively, were observed in all samples. These data show the mixed metal oxides present in the calcined precursors are more easily reduced than the corresponding single-metal species present in the calcined precursors of MoP or Ni_2P prepared in the presence of CA.

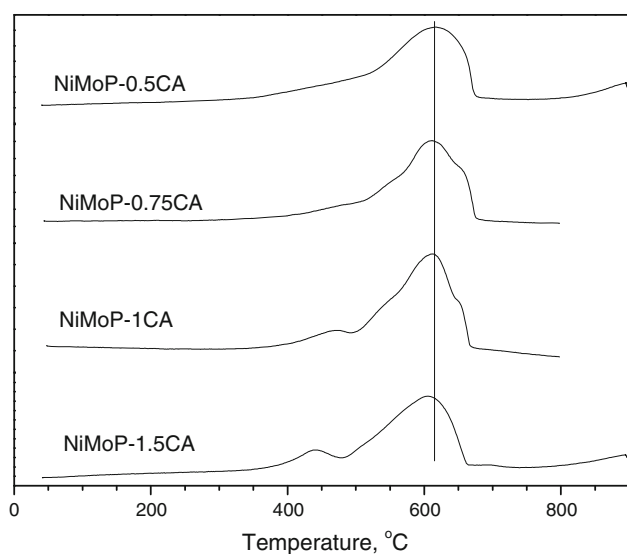


Fig. 5 TPR profiles of catalyst precursors prepared with different CA/Ni ratios

The XPS spectra of the Ni 2p, the Mo 3d and the P 2p regions of the passivated NiMoP catalysts were very similar (not shown) with the major peak binding energies (BEs) summarized in Table 3. In all cases, the spectra were indicative of reduced metal phosphide species, with some oxidized Ni, Mo and P species also apparent due to the presence of the passivation layer on the NiMoP. Peaks at 853.8, 228.2 and 130.4 eV were ascribed to the $\text{Ni}^{\delta+}$ ($0 < \delta < 2$), $\text{Mo}^{\delta+}$ ($0 < \delta < 6$) and $\text{P}^{\delta-}$ ($0 < \delta < 1$), respectively, and no significant shift in BE was observed as the preparation conditions for the reduced, passivated metal phosphide catalysts were varied. The measured catalyst surface compositions determined by XPS (Table 3) show P rich surfaces in all cases, as has been reported previously for most metal phosphides [5, 7, 20]. Also, the data show that the surface P/Me ratio (Me = Ni + Mo) increased gradually with decreased reduction temperature, a consequence of more P loss at higher reduction temperatures. Most significant, however, is the increased P/Me ratio and Ni/Mo ratio as the P content of the precursors increased, and this increase follows the formation of the NiMoP_2 phase identified by XRD.

3.2 HDS of 4,6-DMDBT

The hydrodesulfurization (HDS) of 4,6-DMDBT was performed at 310 °C, 3.0 MPa, and Table 4 reports the HDS conversions obtained over the NiMoP catalysts initially and after 5 h time-on-stream. The 4,6-DMDBT initial conversion decreased significantly with increased reduction temperature and the initial conversion of NiMoP-550

Table 3 Summary of XPS analysis of the reduced metal phosphide catalysts

Catalyst	Binding energy			Surface composition		
	Ni _{2p}	Mo _{3d}	P _{2p}	Nominal P/Me Atomic ratio	Surface Ni/Mo	Surface P/Me
	eV					
NiMoP-1P	854.2	228.7	129.8	1	1.08	1.54
NiMoP-0.75P	853.8	228.3	130.1	0.75	2.86	1.52
NiMoP-0.5P	853.9	228.2	130.2	0.5	0.67	0.79
NiMoP-1.5CA	853.8	228.2	130.2	0.5	0.85	0.72
NiMoP-1CA	853.9	228.2	130.2	0.5	0.67	0.79
NiMoP-0.75CA	853.8	228.4	130.4	0.5	0.67	0.86
NiMoP-0.5CA	853.9	228.3	130.3	0.5	0.67	0.88
NiMoP-650	853.8	228.4	130.4	0.5	0.67	0.79
NiMoP-600	853.9	228.3	130.3	0.5	0.65	0.89
NiMoP-550	854.0	228.2	130.4	0.5	0.62	0.97

catalyst was 79.1 %, similar to that of Ni_2P prepared with CA, as reported previously [6]. For the phase pure NiMoP catalysts (NiMoP-500 and NiMoP-600) the TOFs were almost identical, despite large differences in NiMoP surface areas and crystallite size. Among the catalysts tested, they were the most active in terms of 4,6-DMDBT conversion per unit mass of catalyst.

Table 4 also shows that the initial HDS activity increased with increased P/Me ratio from 0.5 to 1, corresponding to an increase in CO uptake, despite a lower BET area. However, in this case, there was a significant phase change in the prepared catalysts. At a P/Me = 1, NiMoP_2 was the dominant phase rather than NiMoP. The higher TOF observed with increased P content is likely related to the presence of the NiMoP_2 phase. The crystal structure of NiMoP is similar to that of Ni_2P , with the Ni atoms near the center of the side faces of the unit cell replaced by Mo. However, NiMoP_2 has a different crystal structure and a higher P content compared to NiMoP [21], yielding a higher metal-P coordination, that should reduce adsorption of the reactant molecule. Nagai et al. [22] reported that Ni and Ni^{2+} species in Ni-Mo-P/ Al_2O_3 increased during reduction and nickel migrated to the surface and promoted the HDS activity. The high surface Ni/(Ni + Mo) ratio of the NiMoP-1P catalyst of the present study also contributes to the high TOF compared to the NiMoP-0.5P catalyst. The

Table 4 CO uptake and 4,6-DMDBT HDS performance over different catalysts

Catalyst	CO uptake ($\mu\text{mol/g}$)	Initial conv. (%)	Final conv. (%)	TOF (10^{-3} s^{-1})	Selectivity				(TH + HH)/ MCHT Ratio	MCHT/ DMBP
					THDMDBT + HHDMDDBT %	DMBP	MCHT	DMBCH		
NiMoP- 2P	8.3	38.3	43.0	7.0	41.7	12.9	39.0	6.5	1.07	3.00
NiMoP- 1P	7.1	31.9	28.9	5.5	16.0	16.0	51.9	6.1	0.31	3.24
NiMoP- 3CA	0.5	37.3	27.2	2.4	19.0	16.7	64.4	–	0.3	3.87
NiMoP- 2CA	7.1	31.9	28.9	5.5	16.0	16.0	51.9	6.1	0.31	3.24
NiMoP- 1.5CA	19.6	44.1	35.1	3.1	10.4	18.1	67.4	–	0.15	3.72
NiMoP- 1CA	–	45.5	21.0	–	23.2	18.4	58.4	–	0.4	3.23
NiMoP- 1.5CA- 650	19.6	44.1	35.1	3.1	10.4	18.1	67.4	–	0.15	3.72
NiMoP- 1.5CA- 600	19.1	58.8	22.5	4.7	20.8	18.8	61.9	4.3	0.34	3.3
NiMoP- 1.5CA- 550	32.6	79.1	26.4	4.9	12.3	22.2	52.3	12.5	0.24	2.34
Ni ₂ P from [5]	30.1	87.7	80.6	7.1	4.2	8.5	66.6	19.3	0.06	7.83
MoP from [5]	42.4	74.7	34.3	3.3	12.2	12.2	52.3	22.8	0.23	4.28

Reaction conditions: temperature 310 °C, pressure 3.0 MPa H₂, 3,000 ppm 4,6-DMDBT and WHSV 26 h⁻¹

THDMDBT 4,6-tetrahydrodimethyldibenzothiophene, HHDMDDBT hexahydrodimethyldibenzothiophene

data of Table 4 also show that the TOF of the most active NiMoP preparation was comparable to that reported previously for Ni₂P prepared in the presence of CA [5].

The reaction network of 4,6-DMDBT involves two parallel reactions that lead to desulfurized products [23]. One is denoted as direct desulfurization (DDS) which in the case of 4,6-DMDBT results in the formation of 3,3-dimethylbiphenyl (3,3-DMBP). The second, referred to as the hydrogenation pathway (HYD), involves the prehydrogenation of 4,6-DMDBT to 4,6-tetrahydro- and hexahydro-dimethyldibenzothiophenes (THDMDBT and HHDMDDBT), which are subsequently desulfurized to methylcyclohexyltoluene (MCHT) and dimethylbicyclohexane (DMBCH). In the present study, the high ratio of the principal products of the HYD to DDS routes (MCHT/DMBP) shows that the dominant pathway is via the HYD route for all the catalysts.

It is also found that the MCHT/DMBP ratio of NiMoP catalysts decreased with increase in reduction temperature, consistent with a decrease in the crystallite size of the

NiMoP phase. The possible contribution of the Brønsted acidity of metal phosphides that facilitate the DDS pathway of HDS of 4,6-DMDBT [9, 10, 20] is less important for the NiMoP-xP catalysts since the DMBP selectivity was only slightly affected by P content. However, the (THDMDBT + HHDMDDBT)/MCHT ratio increased as the P content increased, suggesting that the NiMoP₂ phase decreased the rate of sulfur elimination from hydrogenated intermediates of the HYD route.

4 Conclusion

The effect of preparation conditions on the structure and catalytic performance of unsupported NiMoP catalysts in the presence of CA has been investigated. The chemical composition and surface area of the NiMoP catalysts was varied by the synthesis conditions, with small amounts of MoP and NiMoP₂ present in some of the catalysts. Chelating Mo and Ni with citric acid suppressed the

aggregation of the catalyst precursors and yielded precursors chemically similar to those identified for MoP and Ni₂P. Phase pure, high surface area NiMoP was synthesized in the presence of CA at low reduction temperature (550 °C), with a Ni/Mo/P ratio of 1/1/1 and a 1.5 CA/Me ratio (Me = Ni + Mo), resulting in a high initial conversion of 4,6-DMDBT, similar to that of Ni₂P prepared with CA. For the phase pure NiMoP catalysts, the TOFs for the HDS of 4,6-DMDBT were almost identical, despite large differences in NiMoP surface areas and crystallite size.

Acknowledgments Financial support from the Natural Sciences and Engineering Research Council of Canada is gratefully acknowledged.

References

- Li W, Dhandapani B, Oyama ST (1998) *Chem Lett* 27:207–208
- Stinner C, Prins R, Weber T (2000) *J Catal* 191:438–444
- Wang X, Clark P, Oyama ST (2002) *J Catal* 208:321–331
- Stinner C, Prins R, Weber T (2001) *J Catal* 202:187–194
- Wang R, Smith KJ (2009) *Appl Catal A* 361:18–25
- Wang R, Smith KJ (2010) *Appl Catal A* 380:149–164
- Whiffen VML, Smith KJ, Straus SK (2012) *Appl Catal A* 419–420:111–125
- Topsøe H, Clausen BS, Massoth FE (1996) In: Anderson JR, Boudart M (eds) *Catalysis science and technology*, vol 11. Springer, Berlin, p 162
- Abu II, Smith KJ (2006) *J Catal* 241:356–366
- Abu II, Smith KJ (2007) *Catal Today* 125:248–255
- Sun F, Wu W, Wu Z, Guo J, Wei Z, Yang Y, Jiang Z, Tian F, Li C (2004) *J Catal* 228:298–310
- Li K, Wang R, Chen J (2011) *Energy Fuels* 25:854–863
- Gaudette AF, Burns AW, Hayes JR, Smith MC, Bowker RH, Seda T, Bussell ME (2010) *J Catal* 272:18–27
- Lee SY, Lee YK, Oyama ST, Lee SH, Woo HC (2007) *Solid State Phenom* 124–126:1765–1768
- Whiffen VL, Smith K (2012) *Top Catal* 55:981–990
- Ma D, Xiao T, Xie S, Zhou W, Gonzalez-Cortes S, Green MLH (2004) *Chem Mater* 16:2697–2699
- Takahashi R, Sato S, Sodesawa T, Suzuki M, Ichikuni N (2003) *Microporous Mesoporous Mater* 66:197–208
- Cheng R, Shu Y, Li L, Zheng M, Wang X, Wang A, Zhang T (2007) *Appl Catal A* 316:160–168
- Arai Y, Sparks DL (2001) *J Colloid Interface Sci* 241:317–326
- Prins R, Bussell M (2012) *Catal Lett* 142:1413–1436
- Oryshchyn SV, Zhak OV, Guérin P, Députier S, Kuźma YB (2002) *Inorg Mater* 38:1195–1202
- Nagai M, Fukiage T, Kurata S (2005) *Catal Today* 106:201–205
- Whitehurst DD, Isoda T, Mochida I (1998) *Adv Catal* 42:345–471